
Discover Generics
Cost-Effective CT & MRI Contrast Agents
FRESENIUS KABI
WATCH VIDEO

AJNR

Why do ulcerated atherosclerotic carotid artery plaques embolize? A flow dynamics study.

S G Imbesi and C W Kerber

AJNR Am J Neuroradiol 1998, 19 (4) 761-766
http://www.ajnr.org/content/19/4/761

This information is current as of June 23, 2025.

AJNR Am J Neuroradiol 19:761–766, April 1998

Why Do Ulcerated Atherosclerotic Carotid Artery Plaques Embolize? A Flow Dynamics Study

Steven G. Imbesi and Charles W. Kerber

PURPOSE: **We describe and analyze flow dynamics and pressure relationships in an ulcerated atherosclerotic human carotid bulb.**

METHODS: **Replicas of an ulcerated atherosclerotic human carotid bulb were created using the lost wax technique. The resulting replicas were placed in a circuit of pulsating non-Newtonian fluid and flows were adjusted to replicate human physiological flow profiles. Common carotid artery total flow volumes of 400, 600, and 800 mL/min were studied. Slipstreams were opacified with isobaric dyes. Images were recorded on 35 mm film and on super VHS video. A pressure recording device was calibrated; data were received from needles placed radially and longitudinally in the common carotid artery, narrowed bulb/ulcer, and internal carotid artery. Multiple pressure recordings were obtained in the replicas.**

RESULTS: **Measurements of the replica showed a 59% diameter stenosis and an 88% area stenosis of the carotid bulb with a shallow 3.3-mm ulcer. Analysis of flow in the common carotid artery showed undisturbed slipstreams, but as these streams entered the narrowed carotid bulb they crowded together and accelerated significantly. This accelerated jet continued for at least two vessel diameters into the more normal portions of the internal carotid artery, where flow remained disturbed peripherally and often assumed a helical pattern but was nonturbulent. As fluid entered the narrowed bulb, radial pressures decreased. Most important, at peak systole, lower radial pressure with a vortex circulation was found at the ulceration.**

CONCLUSION: **This combination of events (ie, slowly swirling fluid within the ulcer, allowing platelet aggregates to form, and the intermittent Bernoulli effect, pulling the aggregates into the rapidly flowing blood) may help explain how ulcerated carotid plaques lead to embolic stroke.**

Flow dynamics in the carotid artery have been described previously (1–8). However, direct pressure measurements in a narrowed carotid arterial system, as well as the flow dynamics and pressure relationships in ulcerated atherosclerotic plaques, have not been studied extensively. Recently, we obtained a fresh cadaveric specimen of an ulcerated, stenotic carotid bulb and made accurate castings and reproductions of that arterial system. We then studied the flow dynamics and pressure relationships in a replica-based model of the system. The results of those experiments are reported herein.

Received May 1, 1997; accepted after revision October 1.

Presented at the annual meeting of the American Society of Neuroradiology, Toronto, Canada, May 1997, where it was awarded the 1997 Cornelius G. Dyke Memorial Award.

From the Department of Radiology, University of California, Davis Medical Center, Sacramento, California (S.G.I.) and the Department of Radiology, University of California, San Diego Medical Center, San Diego, California (C.W.K.).

Address reprint requests to Charles W. Kerber, MD, Department of Radiology, University of California, San Diego, Medical Center, 200 W Arbor Dr, MC 8756, San Diego, CA 92103.

© American Society of Neuroradiology

Methods

We created a casting of an ulcerated atherosclerotic carotid bulb from a fresh human cadaver using the lost wax technique. Details of this process have been described previously (9, 10). Multiple clear elastic silicone replicas made from the original casting were placed in a circuit of pulsatile non-Newtonian fluid (11, 12). A blood pump (model 1421 Harvard apparatus, S Natick, Mass) cycling at one pulse per second provided fluid flow. Flows were adjusted with a Square Wave Electromagnetic Flowmeter (Carolina Medical Electronics; King, NC) to replicate human physiological flow profiles, so that the internal carotid artery had 40% diastolic flow while, during diastole, flow in the external carotid artery fell to zero. We studied common carotid artery flow volumes of 400, 600, and 800 mL/min, representing low-, normal-, and high-flow physiological states, respectively. The proximal internal carotid artery stenosis resulted in 50% of the total flow passing into the internal carotid artery and 50% passing into the external carotid artery. The fluid slipstreams were opacified with isobaric dyes, and images were recorded on 35-mm film and on super VHS video at shutter speeds of 1/1000 second. We then calibrated a pressure recording device (Tektronix #414 Dual Pres-

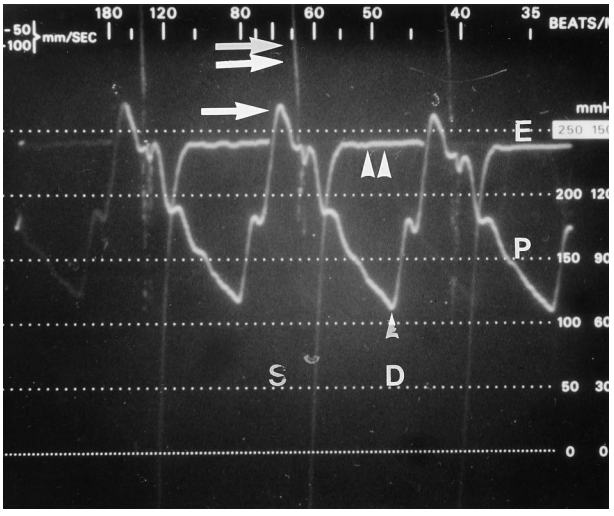

FIG 1. Recorded pressure tracings synchronized to an electrocardiograph show increased pressure (*single arrow*) during systole (*double arrows*) and decreased pressure (*single arrowhead*) during diastole (*double arrowheads*) (*E* indicates electrocardiograph tracing; *P*, pressure tracing; *S*, systole; *D*, diastole).

sure Opt. 21; Beaverton, Ore) in the flowing fluid and synchronized it to the blood pump via an electrocardiograph monitor (Tektronix) to show peak systole (Fig 1).

Twenty-three–gauge needles were attached to the pressure recorder and placed both radially and longitudinally to impinge on different flowing slipstreams. The radial pressure is the pressure perpendicular to the long axis of the vessel and the longitudinal pressure is the pressure parallel to the long axis of the vessel. Radial recordings were made at three locations: the common carotid artery, the internal carotid artery, and the atherosclerotic ulcer. Longitudinal recordings were also taken at the stenosis with the needle tip facing into the flowing fluid (known as a dynamic pressure) and again with the needle tip facing in the direction of the flowing fluid (Fig 2).

Results

In this description, the internal carotid artery is considered a posterior structure, the external carotid artery an anterior structure. The arterial replicas reproduced the original dimensions of the cadaveric specimen to within 1%.

Measurements

Diameters of the vascular cast were measured through two axes at the following locations: the com-

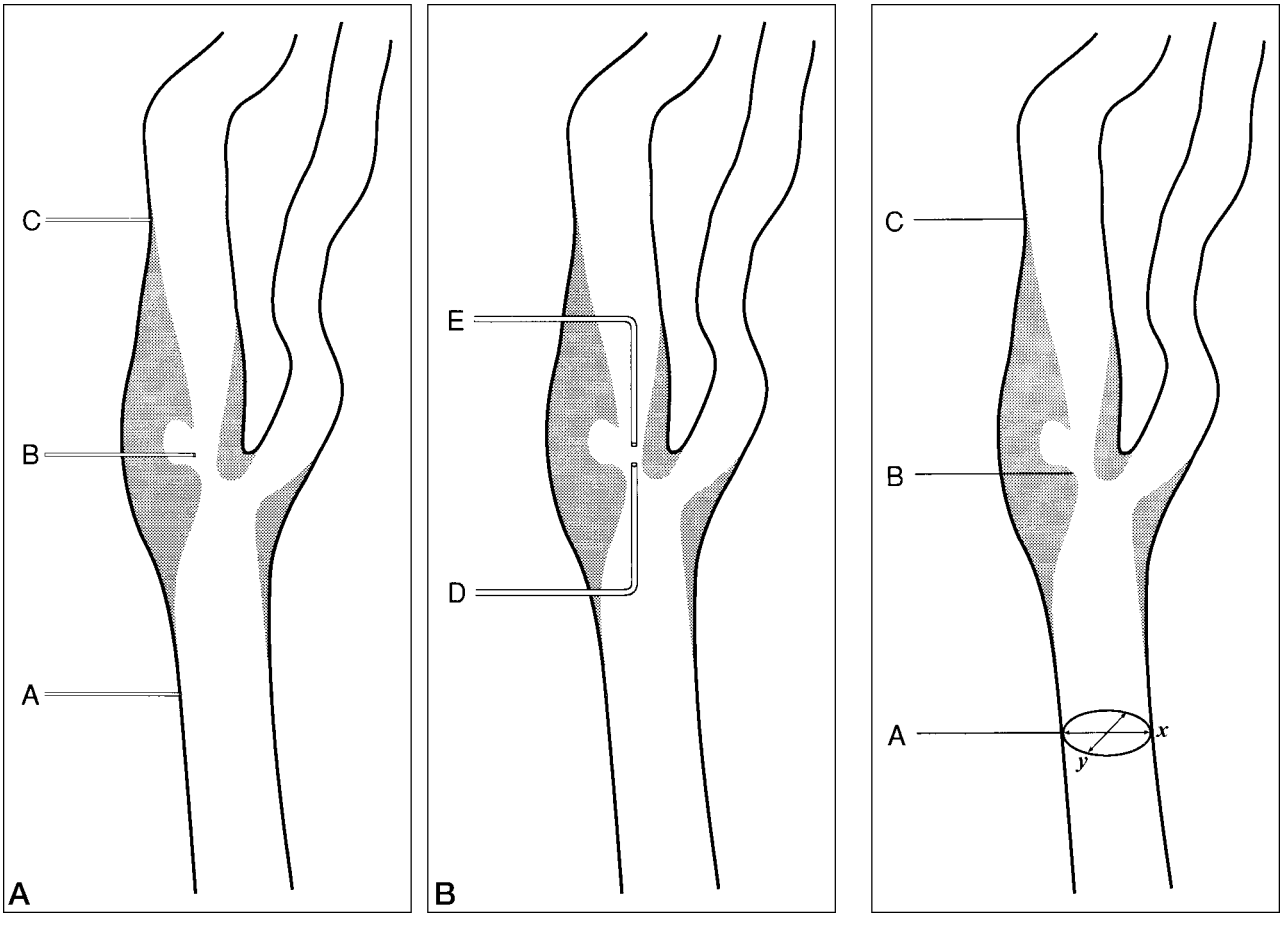

FIG 2. *A*, Needle tip placements during radial pressure recordings (*A* indicates common carotid artery; *B*, stenotic ulcerated bulb; *C*, internal carotid artery).

B, Needle tip placements during longitudinal pressure recordings (*D* indicates with the flow at the stenosis; *E*, against the flow at the stenosis).

FIG 3. Drawing illustrates *x*- and *y*-axis diameter measurements of the common carotid artery (*A*), carotid bulb stenosis (*B*), and internal carotid artery (*C*).

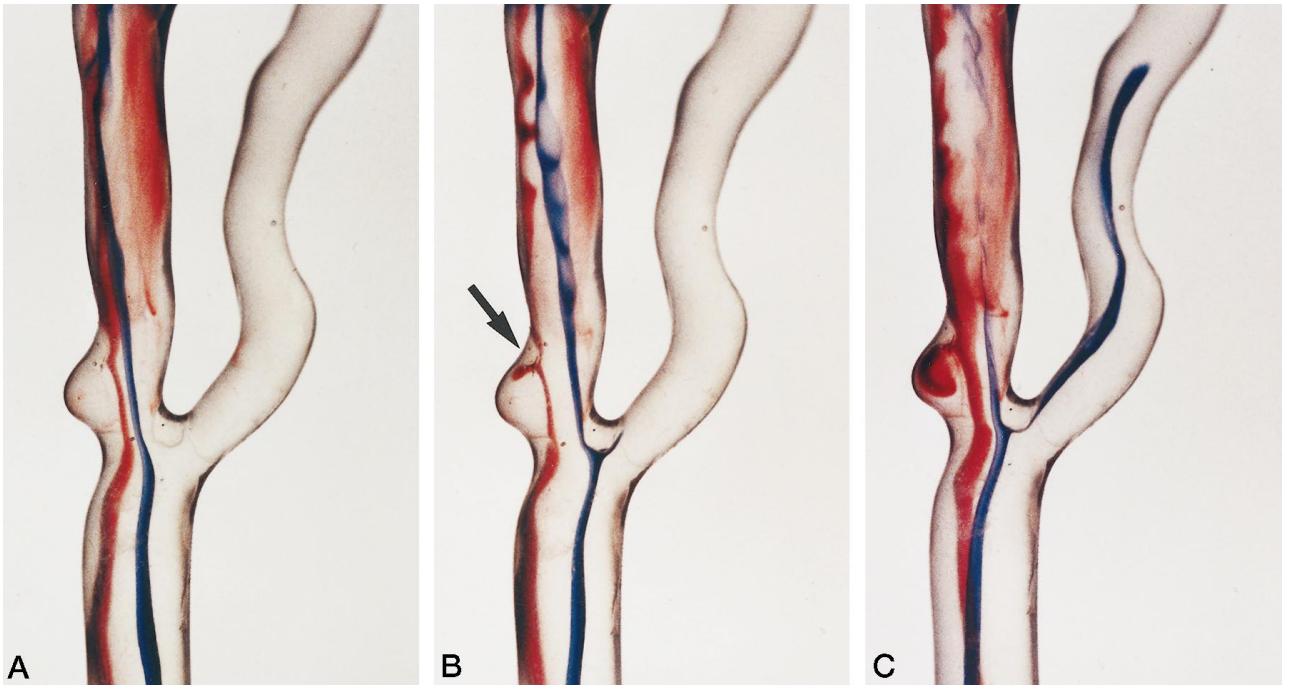

FIG 4. Stenotic carotid bulb and ulcer entry flow analysis.

A, Systole (prior to ulcer slipstream entry): the opacified slipstreams crowd together and accelerate through the carotid bulb stenosis continuing along the posterior wall of the internal carotid artery for a distance of two to three vessel diameters.

B, Diastole: there is less acceleration and therefore less slipstream crowding at the stenosis, which allows slipstream entry into the distal neck of the ulceration (*arrow*). Also note the peripherally disturbed but nonturbulent slipstreams in the internal carotid artery; these slipstreams assume a helical pattern at the distal arterial curvature. The majority of the disturbed, eddying slipstreams are oriented anteriorly.

C, Systole (following ulcer slipstream entry): sluggish swirling slipstreams in a vortex pattern are seen during systole within the ulceration.

mon carotid artery measured 7.04 × 7.38 mm; the narrowest portion of the carotid bulb, 2.70 × 2.30 mm; and the internal carotid artery, 5.38 × 5.63 mm (Fig 3). The ulcer was shallow, measuring 4.95 mm long, 2.90 mm wide, and 3.30 mm deep. Using the formula for an ellipse, we found that these values equated to a 59% diameter stenosis of the carotid bulb by North American Symptomatic Carotid Endarterectomy Trial (NASCET) criteria, using the internal carotid artery as a reference, and an 88% area stenosis of the carotid bulb using the common carotid artery as a reference.

Flow

Analysis of flow in the common carotid artery showed undisturbed slipstreams parallel to the vessel side wall. These slipstreams were of generally equal velocity. As slipstreams entered the narrowed bulb, they crowded together and accelerated. Beyond the narrowing, a central high-velocity jet continued for a distance of two to three vessel diameters, mostly along the posterior wall. Flow in the immediate poststenotic segment was disturbed around the periphery of the jet, eddying mostly anteriorly. As the dye streams passed distally into the internal carotid artery, they regained a more normal entry zone profile but also often assumed a helical pattern. Some fluid slipstreams entered the distal opening of the ulcer, swirled along the plaque wall opposite the direction of normal flow, and exited via the proximal opening of the ulcer (Figs 4 and 5).

Pressure

Pressure recordings throughout the cardiac cycle synchronized to peak systole at flow volumes of 400, 600, and 800 mL/min yielded the results in Table 1 for radial pressures and those in Table 2 for longitudinal pressures. The radial pressures were obtained at the common carotid artery, the narrowed bulb/ulcerated plaque, and the internal carotid artery. The longitudinal pressures were measured at the stenosis. As fluid entered the narrowing and accelerated, radial pressures fell, especially during peak systole. The same inverse radial pressure-to-velocity relationships continued for at least two vessel diameters downstream beyond the narrowing, although to a lesser degree. Most important, at peak systole, low radial pressure with a sluggish vortex circulation was found at the ulceration. Measurement of longitudinal pressures showed dependency on flow direction. The pressures increased when the needle tip was facing into the flowing fluid as compared with pressures measured at the same point when the needle tip was facing in the direction of flow. These findings were not apparent at the lower flow volume of 400 mL/min,

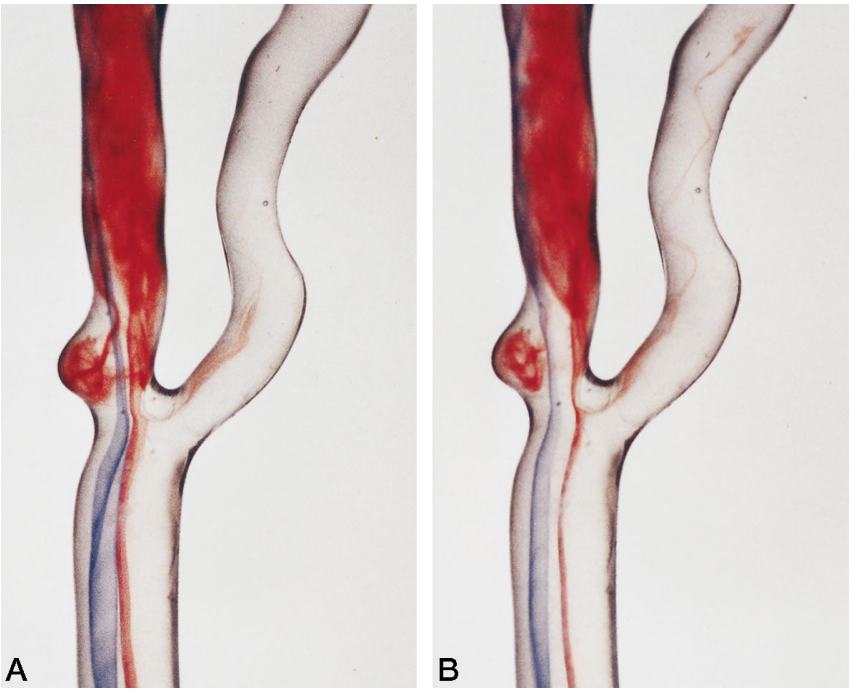

FIG 5. Stenotic carotid bulb and ulcer exit flow analysis.

A, Systole: a series of images with injections into different slipstreams than in Figure 4 shows an opacified slipstream exiting the proximal part of the neck of the ulcer and being sucked into the central jet of the stenosis.

B, Diastole: continued sluggish swirling flow in a vortex pattern is also seen during diastole within the ulceration.

TABLE 1: Radial pressures: peak systole/peak diastole

		Vessel Segment		
		CCA	Ulcer	ICA
Q	400	26/14	21/10	21/11
	600	43/22	27/16	34/17
	800	52/23	39/16	44/22

Note.—Q indicates flow in mL/min; CCA, common carotid artery; Ulcer, ulcerated atherosclerotic bulb; ICA, internal carotid artery; pressures measured in centimeters of water (cm H_2O).

but their relationships became obvious at the higher flow volumes of 600 and 800 mL/min.

Discussion

Hemodynamics is the study of the movement of blood and of the forces concerned therein (13). Although angiography provides superb anatomic detail of normal and stenotic carotid arterial systems, it does not provide physiological data. Duplex Doppler sonography and magnetic resonance angiography do provide some physiological information, but flow of individual slipstreams and the resultant pressure changes cannot be measured by these techniques. The use of clear elastic silicone vascular replicas from human cadaveric sources provides the means for making high-resolution detailed analyses of individual slipstream flow profiles and also enables direct in vitro analysis of corresponding physiological forces, such as pressures. An understanding of these forces gives us insight into the resultant pathologic processes.

While the total pressure in a system containing flowing fluid is constant, the radial and longitudinal pressures change inversely and proportionally depending on the velocity of the fluid as described by the following equations (14, 15).

$A_1 v_1 = A_2 v_2$ [equation(Eq) 1] where

A = cross-sectional area

and v = fluid velocity

$P_1 + 1/2\ \rho v_1^2 = P_2 + 1/2\ \rho v_2^2$ [Eq 2] where

P = radial pressure,

ρ = fluid viscosity,

v = fluid velocity, and

$1/2\ \rho v^2$ = longitudinal pressure

Therefore, in a Newtonian system, as arterial cross-sectional area decreases, the fluid velocity increases, the longitudinal pressure increases, and subsequently the radial pressure decreases (eg, if $A_2<A_1$, then $v_2>v_1$[Eq 1] and if $v_2>v_1$, then $P_2<P_1$ [Eq2]) (Fig 6). The *radial pressure* is the pressure perpendicular to the long axis of the vessel and is that ordinarily measured by a blood pressure cuff, while the *longitudinal pressure* is the pressure parallel to the long axis of the vessel and is that normally measured by end-hole catheters. The longitudinal pressure is also dependent on the direction of flow; when the orifice of the

TABLE 2: Longitudinal pressures (at the stenosis): peak systole/peak diastole

		Direction of Needle Tip	
		Against the Flow	With the Flow
Q	400	22/11	20/11
	600	41/21	30/16
	800	49/21	40/17

Note.—Q indicates flow in mL/min; pressure measured in centimeters of water (cm H_2O).

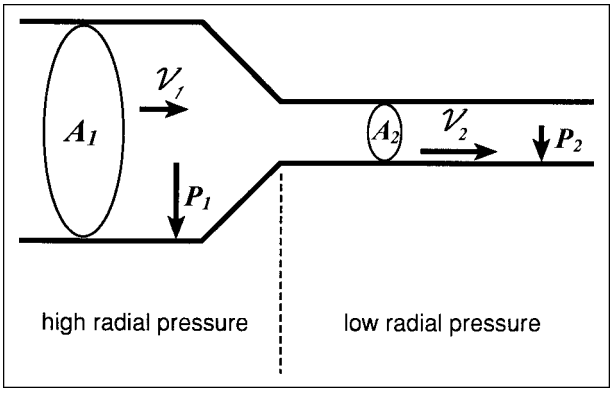

FIG 6. Graphic depiction of area-velocity and velocity-pressure equations. Vector length is proportional to vector magnitude.

catheter faces into the flowing fluid, the measurement is called *dynamic pressure*.

Our observations and interpretations of the data follow. In the common carotid artery, fluid slipstreams were characteristic of the entry zone profile found in humans by Doppler sonography; that is, all velocity vectors were nearly the same except for those near the artery wall's boundary layer (16). At the site of stenosis, the opacified slipstreams crowded together and accelerated. Although the narrowings were moderate to severe, fluid slipstreams in the poststenotic segment, while highly disturbed, remained nonturbulent but often assumed a helical pattern, especially in the regions of vessel curvature. When the radial pressures measured in the common carotid and internal carotid arteries were used as baselines, pressures measured radially in the high-velocity stenotic segment decreased. Specifically, an inverse relationship of marked radial pressure decrease was found at the stenotic, ulcerated bulb during periods of maximal flow velocity (ie, at peak systole). In addition, vortex or reverse swirling flow was noted within the atherosclerotic ulcer cavity. This vortex type of flow has also been observed in vessel side-wall aneurysms (C. W. Kerber, V. Graves, unpublished data). These slipstreams entered the ulcer during diastole and were sucked out of the ulcer during peak systole (Fig 7). Theoretically, this combination of events (slowly swirling fluid allowing platelet aggregates and thrombus to form and the Bernoulli effect sucking the slipstreams and concomitantly pulling aggregates into the adjacent rapidly flowing blood) may help explain how human ulcerated atherosclerotic carotid artery plaques lead to embolic stroke.

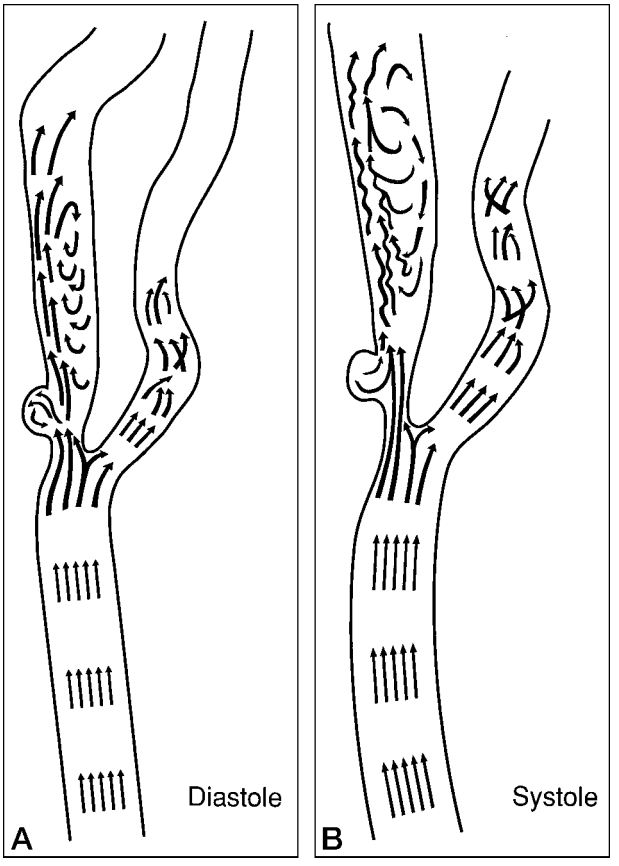

FIG 7. Schematic representations of observed events delineate slipstream entry from the stenotic bulb into the ulcer during diastole (*A*) and slipstream exit from the ulcer into the high-velocity jet of the stenotic bulb during peak systole (*B*). Sluggish vortex flow is seen within the ulceration. Vector length is proportional to slipstream velocity.

We also observed differences in longitudinal pressures depending on the relationship between the direction of the needle's end–hole and the direction of flow. Therefore, when an end-hole catheter is used for pressure measurement, consideration of these factors may also be warranted.

Acknowledgment

We gratefully acknowledge Erika E. Edwards for her invaluable assistance in preparing the manuscript.

References

1. Kerber CW, Liepsch D. **Flow dynamics for radiologists, II: practical considerations in the live human.** *AJNR Am J Neuroradiol* 1994;15:1076–1086
2. Motomiya M, Karino T. **Flow patterns in the human carotid artery bifurcation.** *Stroke* 1984;15:50–56
3. Ku DN, Giddens DP. **Pulsatile flow in a model carotid bifurcation.** *Arteriosclerosis* 1983;3:31–39
4. Fox JA, Hugh AE. **Static zones in the internal carotid artery: correlation with boundary layer separation and stasis in model flows.** *Br J Radiol* 1976;43:370–376
5. Dewey CF. **Fluid mechanics of arterial flow.** *Adv Exp Med Biol* 1979;115:55–104
6. Bharadvaj BK, Mabon RF, Giddens DP. **Steady flow in a model of the human carotid bifurcation, I: flow visualization.** *J Biomech*

1982;15:349–362
7. Karino T, Goldsmith HL, Motomiya M, Mabuchi S, Sohara Y. **Flow patters in vessels of simple and complex geometries.** *Ann N Y Acad Sci* 1987;516:422–441
8. Kerber CW, Knox K, Hecht ST, Buxton RB. **Flow dynamics in the human carotid bulb.** *Int J Neuroradiol* 1996;2:422–429
9. Kerber CW, Heilman CB, Zanetti PH. **Transparent elastic arterial models, I: a brief technical note.** *Biorheology* 1989;26: 1041–1049
10. Liepsch D, Zimmer R. **A method for the preparation of true-to-scale inflexible and natural elastic human arteries.** *Biomed Tech* 1978;23:227–230
11. Mann DE, Tarbell JM. **Flow of non-Newtonian blood analog fluids in rigid curved and straight artery models.** *Biorheology* 1990;27: 711–733
12. Liepsch D, Morabec ST. **Pulsatile flow of non-Newtonian fluid in distensible models of human arteries.** *Biorheology* 1984;21:571–586
13. *Dorland s Illustrated Medical Dictionary.* 28th ed. Philadelphia, Pa: Saunders; 1994:748
14. Berne RM, Levy MN. **Hemodynamics.** In: *Physiology.* St Louis, Mo: Mosby; 1983:473–484
15. Serway RA. *Physics for Scientists & Engineers.* 4th ed. Philadelphia, Pa: Saunders; 1996:433–435
16. Keller HM, Merer WE, Anliker M, et al. **Noninvasive measurement of velocity profiles and blood flow in the common carotid artery by pulsed Doppler ultrasound.** *Stroke* 1976;7:370–377